International Journal of Applied Engineering Research ISSN 0973-4562 Volume 10, Number 18 (2015) pp 38873-38879

Development of a Three Dimensional Code based on Diluted Perfect Difference and Multi-Diagonal Codes for OCDMA Systems

Rasim Azeez Kadhim
PG Scholar, School of Computer and Communication Engineering, Universiti Malaysia Perlis (UniMap), Pauh Putra, Arau, Perlis 02600, Malaysia. Ministry of Sciences and Technology, Baghdad, Iraq rasmaziz@yahoo.com

Hilal Adnan Fadhil,
Dr., School of Computer and Communication Engineering, Universiti Malaysia Perlis (UniMap), Pauh Putra, Arau, Perlis 02600, Malaysia hilaladnan@unimap.edu.my

S. A. Aljunid,
Professor Dr., School of Computer and Communication Engineering, Universiti Malaysia Perlis (UniMap), Pauh Putra, Arau, Perlis 02600, Malaysia syedalwee@unimap.edu.my

Mohamad Shahrazel Razalli
Dr. School of Computer and Communication Engineering, Universiti Malaysia Perlis (UniMap), Pauh Putra, Arau, Perlis 02600, Malaysia shahrazel@unimap.edu.my

Abstract
In this paper, a new family of three dimensional codes named three dimensional diluted perfect difference/multi diagonal (3-D DPD/MD) code is proposed. The corresponding architecture for spectral/time/spatial optical code division multiple access (OCDMA) system also is presented. The construction of this code based on multi-diagonal (MD) code for spatial domain and diluted perfect difference (DPD) codes for spectral and time domains. The proposed code has the property of multi-access interference (MAI) cancellation. The system is compared with other systems using; 2-D perfect difference (2-D PD) code, 2-D DPD code, and 3-D perfect difference (3-D PD) code. The numerical results revealed that the proposed system can accommodate much more of active users at a bit error rate (BER) of (10^{-9}) and data rate of 0.622Gbps and 1.25Gbps. Not only does the proposed system has a better performance, but the receiver structure is simpler than the 3-D PD code system where the complexity is reduced to less than 50%.

Keywords: Diluted Perfect Difference (DPD) Codes, Optical Code Division Multiple Access (OCDMA), Perfect Difference (PD) Codes, Phase-Induced Intensity Noise (PIIN).

Introduction

Over the last two decades, the optical code division multiple access (OCDMA) systems have been investigated by many researchers because these systems help multiple users to simultaneously access the same bandwidth with secure communication. Initially, the incoherent OCDMA systems have been proposed based on the intensity modulation and direct detection (IM/DD) for simplicity and lowering cost. The first trials of coding were usually based on the time spreading [1]–[3]. Chung et.al., [1] proposed the optical orthogonal code (OOC) for time spreading, however, the code length was long and the system performance was degraded by the interference from other simultaneous users, called multiple-access interference (MAI) or multiple-users interference (MUI). Weng and Wu proposed the perfect difference (PD) code which had fixed in phase cross correlation (IPCC) property to eliminate the MAI and reduce the code length. On the other hand, the spectral amplitude coding optical code division multiple access (SAC-OCDMA) systems have been presented by exploiting the frequency (wavelength) domain to represent the codes of users [4]–[9]. In addition to the MAI, the phase-induced intensity noise (PIIN) is a dominant noise in such systems. In [6], Zou *et al.*, proposed the modified quadratic congruence (MQC) code with IPCC equal to one to mitigate the effect of MAI and PIIN using a complementary detection technique at the receiver. In [9], Abd et al., presented the multi diagonal (MD) code for SAC-OCDMA system with zero IPCC for fully elimination of MAI and PIIN. The code length was too long to accommodate a large number of users. This is a main obstacle in the one dimension (1-D) coding.

The combinations of two dimensions (2-D) (time/spectral, spectral/spatial, time/spatial) codes were proposed to override the obstacle of 1-D codes [10]–[13]. These 2-D codes enhance the system performance by increasing the number of simultaneous users and mitigating the PIIN. Lin *et al.*, [11], proposed 2-D perfect difference (2-D PD) codes. The number of simultaneous users and the total transmission rate increased significantly. Yeh *et al.*, [13] developed the 2-D diluted perfect difference (2-D DPD) codes based on both the PD code and the dilution method and presented transceiver structures that were fully eliminated MAI.

To increase the number of users, Yeh *et al.* [14], proposed 3-D perfect difference (3-D PD) codes with the structure of a spectral/time/spatial OCDMA system. Numerical results have shown further suppression of the PIIN and an increase in the number of simultaneous users compared with those of previous codes with the same total code length.

In this paper, a new 3-D code is proposed to improve the performance of the 3-D PD code. The mathematical expression for the BER of the proposed code is derived. The

effects of PIIN, shot noise, and thermal noise are considered. Subsequently, the performance of the proposed code is compared with that of traditional codes, such as the 2-D PD, 2-D DPD and 3D-PD codes. Numerical results verified that the proposed system has a superior performance than the best system that used the 3-D PD code at bit rates of 0.622Gbps and 1.25Gbps.

The rest of this paper is organized as follows. Section 2 explains the construction of the 3-D DPD/MD codes. Section 3 presents the structures of both transmitter and receiver of the proposed system. The analytical analysis of the system performance based on the proposed code is derived in Section 4. The comparisons of analytical results and discussions are illustrated in Section 5. Finally, the conclusions are drawn in Section 6.

3-D DPD/MD Code Construction

The construction of the 3-D DPD/MD codes depends on the MD code [9], and the DPD codes which constructed by applying the dilution method on the PD code [13]. The MD code is used for spatial domain and two DPD codes are used for spectral and time domains. Let X and Y are two PD codes where $X = \{x_0, x_1, \dots, x_{M-1}\}$ and $Y = \{y_0, y_1, \dots, y_{N-1}\}$ with the code lengths $M = w_1^2 - w_1 + 1, N = w_2^2 - w_2 + 1$ where w_1 and w_2 are the code weights of X and Y, respectively. The diluted sequences of X and Y are XD and YD that can be constructed by inserting $m-1$ and $n-1$ zeros after each entry of X and Y, where m and n are the extending factors of X and Y, respectively [13].

$$\begin{aligned} XD &= \{x_0, 0, \dots, 0, x_1, 0, \dots, 0, \dots, x_{M-1}, 0, \dots, 0,\} \\ &= \{x_{D0}, x_{D1}, \dots\dots, x_{DM-1}\} \\ YD &= \{y_0, 0, \dots, 0, y_1, 0, \dots, 0, \dots, y_{M-1}, 0, \dots, 0,\} \\ &= \{y_{D0}, y_{D1}, \dots\dots, y_{DM-1}\} \end{aligned} \quad (1)$$

The DPD codes have the same weights as the original PD codes but the lengths and the sizes are $M_D = mM$, and $N_D = nN$. The cyclic shifted versions of XD and YD are XD_e and YD_f which can be obtained by shifting XD and YD for e and f times, respectively where $e = 0, 1, \dots, M_D - 1,$, and $f = 0, 1, \dots, N_D - 1$. Let $Z_l = \{z_{l,0}, z_{l,1}, \dots, z_{l,P-1}\}$ be a set of MD codes with a code length of $P = P_s * w_3$ where w_3 and P_s are the weight and the size of the code, respectively and $l = 0, 1, \dots, P_s - 1$. The system cardinality will be equal to the multiplication of these three code sizes $M_D N_D P_s$.

The expression of the 3-D DPD/MD code is $B_{e,f,l} = XD_e^T YD_f Z_l$, where Z_l is a matrix of Z elements multiplied by the identity matrix of size $N_D \times N_D$. Therefore, $B_{e,f,l}$ can be expressed as in equ. (2). An example of the first codeword of 3-D DPD/MD code with (M_D=2*3, N_D=3*3, and P=4) where XD_0=[101000], YD_0=[100100000] and Z_0=[1001] is shown in TABLE 1.

$$B_{e,f,l} = \begin{bmatrix} b_{0,0,0} & b_{0,1,0} & \dots & b_{0,N_D-1,0} & b_{0,0,1} & b_{0,1,1} & \dots & b_{0,N_D-1,1} & b_{0,0,P-1} & b_{0,1,P-1} & \dots & b_{0,N_D-1,P-1} \\ b_{1,0,0} & b_{1,1,0} & \dots & b_{1,N_D-1,0} & b_{1,0,1} & b_{1,1,1} & \dots & b_{1,N_D-1,1} & b_{1,0,P-1} & b_{1,1,P-1} & \dots & b_{1,N_D-1,P-1} \\ \vdots & & & & & & & & & & & \\ b_{M_D-1,0,0} & b_{M_D-1,1,0} & \dots & b_{M_D-1,N_D-1,0} & b_{M_D-1,0,1} & b_{M_D-1,1,1} & \dots & b_{M_D-1,N_D-1,1} & b_{M_D-1,0,P-1} & b_{M_D-1,1,P-1} & \dots & b_{M_D-1,N_D-1,P-1} \end{bmatrix} \quad (2)$$

To explain the cross correlation of the 3-D PD/MD codes, an eight characteristic matrices $B^a, a \in (0,1,\dots.,7)$ can be introduced as follows:

$$\begin{aligned} B_{e,f,l}^{(0)} &= XD_e^T YD_f Z_l \; B_{e,f,l}^{(1)} = XD_e^T \overline{YD_f} Z_l \\ B_{e,f,l}^{(2)} &= \overline{XD_e^T} YD_f Z_l \; B_{e,f,l}^{(3)} = \overline{XD_e^T} \overline{YD_f} Z_l \\ B_{e,f,l}^{(4)} &= XD_e^T YD_f \bar{Z}_l \; B_{e,f,l}^{(5)} = XD_e^T \overline{YD_f} \bar{Z}_l \\ B_{e,f,l}^{(6)} &= \overline{XD_e^T} YD_f \bar{Z}_l \; B_{e,f,l}^{(7)} = \overline{XD_e^T} \overline{YD_f} \bar{Z}_l \end{aligned} \quad (3)$$

Where $\overline{XD}$ and $\overline{YD}$ are the diluted of the complementary of X and Y, respectively. $\overline{ZD}$ is the diluted of the complementary of Z sequence multiplied each element by the identity matrix of size $N_D \times N_D$. Hence, the cross correlation between the characteristic matrix $B_{e,f,l}^{(a)}$ and any code matrix $B_{e,f,l}$ is defined in equ. 4. The cross correlation properties of the 3-D DPD/MD codes are presented in TABLE 2.

$$R^{(a)}(e,f,l) = \sum_{i=0}^{M_D-1} \sum_{j=0}^{N_D-1} \sum_{h=0}^{P-1} b_{i,j,h}^{(a)} . b_{i,j,h} \quad (4)$$

TABLE 1. A sample codeword of 3D-DPD/MD code with(M_D=6, N_D=9, P=4)

	Z_0=[1 0 0 1]			
XD_0	YD_0=[100100000]	YD_0=[100100000]	YD_0=[100100000]	YD_0=[100100000]
1	100100000	000000000	000000000	100100000
0	000000000	000000000	000000000	000000000
1	100100000	000000000	000000000	100100000
0	000000000	000000000	000000000	000000000
0	000000000	000000000	000000000	000000000
0	000000000	000000000	000000000	000000000

TABLE 2: the cross correlation properties of the 3-D DPD/MD code

	$R^{(0)}(e,f,l)$	$R^{(1)}(e,f,l)$	$R^{(2)}(e,f,l)$	$R^{(3)}(e,f,l)$
e=0∩f=0∩l=0	$w_1w_2w_3$	0	0	0
e=m, 2m,…(M-1)m∩f=0∩l=0	w_2w_3	0	$w_2w_3(w_1-1)$	0
e=0∩f=n, 2n,…(N-1)n∩l=0	w_1w_3	$w_1w_3(w_2-1)$	0	0
e=m, 2m,…(M-1)m ∩ f=n, 2n,…(N-1)n ∩l=0	w_3	$w_3(w_2-1)$	$w_3(w_1-1)$	$w_3(w_2-1)(w_1-1)$
e=0∩f=0∩l≠0	0	0	0	0
e=m, 2m,…(M-1)m∩f=0∩l≠0	0	0	0	0
e=0∩f=n, 2n,…(N-1)n∩l≠0	0	0	0	0
e=m, 2m,…(M-1)m ∩ f=n, 2n,…(N-1)n ∩l≠0	0	0	0	0
Others	0	0	0	0

	$R^{(4)}(e,f,l)$	$R^{(5)}(e,f,l)$	$R^{(6)}(e,f,l)$	$R^{(7)}(e,f,l)$
$e=0 \cap f=0 \cap l=0$	0	0	0	0
$e=m, 2m,\ldots(M-1)m \cap f=0 \cap l=0$	0	0	0	0
$e=0 \cap f=n, 2n,\ldots(N-1)n \cap l=0$	0	0	0	0
$e=m, 2m,\ldots(M-1)m \cap f=n, 2n,\ldots(N-1)n \cap l=0$	0	0	0	0
$e=0 \cap f=0 \cap l\neq 0$	$w_1w_2w_3$	0	0	0
$e=m, 2m,\ldots(M-1)m \cap f=0 \cap l\neq 0$	w_2w_3	0	$w_2w_3(w_1-1)$	0
$e=0 \cap f=n, 2n,\ldots(N-1)n \cap l\neq 0$	w_1w_3	$w_1w_3(w_2-1)$	0	0
$e=m, 2m,\ldots(M-1)m \cap f=n, 2n,\ldots(N-1)n \cap l\neq 0$	w_3	$w_3(w_2-1)$	$w_3(w_1-1)$	$w_3(w_2-1)(w_1-1)$
Others	0	0	0	0

As can be seen from TABLE 2, the cross correlation can be divided into two similar groups: group 1 includes $(R^{(0)}(e,f,l),\ R^{(1)}(e,f,l),\ R^{(2)}(e,f,l),\ R^{(3)}(e,f,l)\ )$; and group 2 includes $(R^{(4)}(e,f,l),\ R^{(5)}(e,f,l),\ R^{(6)}(e,f,l),\ R^{(7)}(e,f,l))$. Therefore, any one of these groups can be used to construct the receiver. The cross correlation at the receiver using group 1 can be expressed as follows:

$$R^{(0)}(e,f,l) - \frac{R^{(1)}(e,f,l)}{(w_2-1)} - \frac{1}{(w_1-1)}\left[R^{(2)}(e,f,l) - \frac{R^{(3)}(e,f,l)}{(w_2-1)}\right] = \begin{cases} w_1w_2w_3 & e=0, f=0, l=0 \\ 0 & otherwise \end{cases} \quad (5)$$

System Description

Fig.1 shows the structure of the transmitter of the proposed system including an incoherent light source, an electrical to optical modulator (EOM) to convert the data bits from electrical form to optical form, w_2 optical delay lines for time spreading, an optical splitter for spatial coding and two sets of fiber brag grating FBGt1 and FBGt2 where they have the same number of gratings but with the opposite arrangement used for spectral coding and run-trip delays compensation, respectively. The incoming data bits were firstly modulated by the EOM in accordance with the ON-OFF keying format, where the electronic signals are converted into optical pulses. Then the modulated optical pulses are delivered to the FBGt1 in order to encode it spectrally according to the spectral code sequence XD_e. Where the spectral components with wavelengths matched to '1' of a code sequence are reflected back and the other filtered out, the reflected spectral components are delivered to the FBGt2 to compensate the run-trip delay.

In order to encode the optical pulses in time, these spectral components were delivered to the optical delay lines. The spectral power is divided into w_2 equal parts and pass through w_2 delay lines with different time delays according to the code sequence YD_f.

Later, these optical pulses reach the optical splitter which are split into w_3 equal parts in order to send it to the couplers according to the code sequence of Z_l. Now the optical signal is fully encoded in three dimensions.

The structure of the receiver is shown in Fig. 2, which comprises one combiner, two correlators, two balanced detectors and an integrator. The incoming optical signals from the couplers are summed up by the combiner according to the code sequence Z_l. In order to dispread the signals in time, the two correlators are used. The correlator 1 consists of w_2 delay lines and the correlator 2 consists of $N - w_2$ delay lines based on the code sequence YD_f and $\overline{YD_f}$, respectively.

Each balanced detector has four sets of FBGs, four circulators, two photodiodes. FBGs r2 and FBGr4 are used to reflect back the same spectral components which are matched to "1s" of the spectral code sequence XD_e. FBG r1 and FBGr3 have the same gratings but in opposite direction to compensate the round-trip delays. FBGs r6 and FBGr8 are used to reflect back the same spectral components which are matched to "1s" of the spectral code sequence of the modified complementary $\overline{XD_e}$. FBGr5 and FBGr7 have the same gratings but in opposite direction to compensate the run-trip delays. Finally, the aggregated signal is integrated by the integrator over the chip period.

According to the equ. (5), the output currents of PDs(0,1,2,3) are respectively proportional to $R^{(0)}(e,f,l)$, $R^{(1)}(e,f,l)/(w_2-1)$, $R^{(2)}(e,f,l)/(w_1-1)$, $R^{(3)}(e,f,l)/(w_2-1)(w_1-1)$.

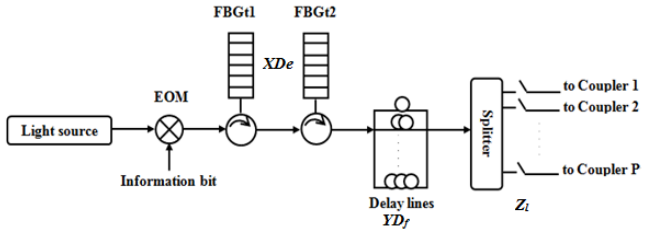

Fig. 1. Transmitter structure of the proposed system

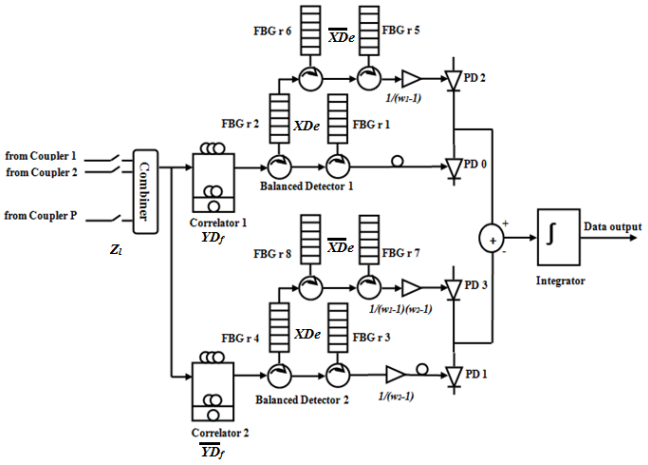

Fig. 2. Receiver structure of the proposed system.

System performance

The system performance is analyzed in terms of a mathematical expression of the signal to noise ratio (SNR) and the bit error rate (BER) with respect to the number of active users at the presence of noise. Three types of noise will be considered in this analysis, which are the shot, *PIIN* and thermal noise. The other noise such as the dark current will be neglected. Gaussian approximation is used in calculation of BER, the variance of noise is [6].

$$< i_{noise}^2 > = < i_{PIIN}^2 > + < i_{shot}^2 > + < i_{thermal}^2 > = B_w I_r^2 \tau_r + 2eB_w I_{total} + \frac{4K_b T_n B_w}{R_L} \quad (6)$$

Where B_w is the electrical noise bandwidth, e is the electron charge, R_L is the load resistance, I_r is the average photocurrent, K_b is Boltzman's constant, I_{total} is the total photocurrent, and τ_r is the coherence time of the light which can be expressed as [6]:

$$\tau_r = \frac{\int_0^\infty S^2(v)dv}{\left[\int_0^\infty S(v)dv\right]^2} \quad (7)$$

Where $S(v)$ is the single sideband power spectral density (PSD).

Four assumptions are made to simplify the analysis [6]:

First, the broadband light source is ideally unpolarized and its spectrum is flat over $[v_0 - \Delta v/2, v_0 + \Delta v/2]$ and emits equal power, where v_0 is the central optical frequency and Δv is the optical source bandwidth. Second, each spectral component produced by the spectral encoders has an identical spectral width. Third, each spectral component received by a user has the same power. Fourth, each bit stream from each user is synchronized. We defined $U(v,i)$ as follows:

$$U(v,i) = \left\{u\left[v - v_0 - \frac{\Delta v}{2M}(-M+2i)\right] - u\left[v - v_0 - \frac{\Delta v}{2M}(-M+2i+2)\right]\right\} \quad (8)$$

Where $u(v)$ is a unit step function defined as:

$$u(v) = \begin{cases} 1 & v \geq 0 \\ 0 & v < 0 \end{cases} \quad (9)$$

Based on the assumptions above, the PSD of the received signals can be written as:

$$r(v) = \frac{P_{sr}}{w_2 w_3 \Delta v} \times \sum_{k=1}^{K} d(k) \sum_{h=0}^{P-1} \sum_{i=0}^{M_D-1} \sum_{j=0}^{N_D-1} b_{(i,j,h)}(k) U(v,i) \quad (10)$$

Where P_{sr} is the effective source power at the receiver, w_1, w_2 and $w_3$are the code weights, K is the number of active users, $d(k)$ is the data bit of *kth* user which can be '1' or '0', M_D, N_D and P are the code lengths of spectral, time spreading and spatial code sequences respectively, and $b_{i,j,h}(k)$ is an element of the *kth* user's codeword.

We will obtain the output currents of PDs (0,1,2,3) at receiver$(0,0,0)$ depending on the cross correlation between $B_{0,0,0}^{(a)}$ and $B_{e,f,l}$ as follows:

$$I_0 = \mathcal{R}\int_0^\infty G_0(v)dv = \int_0^\infty \frac{\mathcal{R}P_{sr}}{w_2 w_3 \Delta v} \times \sum_{k=1}^{K} d(k) R^{(0)}(i,j,h) U(v,i) dv = \frac{\mathcal{R}P_{sr}}{w_2 w_3 M_D}\left\{w_3 w_1 w_2 + \frac{w_2 w_3 (K-1)(M-1)}{(M_D N_D P_s - 1)} + \frac{w_3 w_1 (K-1)(N-1)}{(M_D N_D P_s - 1)} + \frac{w_3 (K-1)(N-1)(M-1)}{(M_D N_D P_s - 1)}\right\} \quad (11)$$

$$I_1 = \mathcal{R}\int_0^\infty G_1(v)dv = \int_0^\infty \frac{\mathcal{R}P_{sr}}{(w_2 - 1) w_2 w_3 \Delta v} \times \sum_{k=1}^{K} d(k) R^{(1)}(i,j,h) U(v,i) dv = \frac{\mathcal{R}P_{sr}}{w_2 w_3 M_D}\left\{\frac{w_3 w_1 (K-1)(N-1)}{(M_D N_D P_s - 1)} + \frac{w_3 (K-1)(N-1)(M-1)}{(M_D N_D P_s - 1)}\right\} \quad (12)$$

$$I_2 = \mathcal{R}\int_0^\infty G_2(v)dv = \int_0^\infty \frac{\mathcal{R}P_{sr}}{(w_1 - 1) w_2 w_3 \Delta v} \times \sum_{k=1}^{K} d(k) R^{(2)}(i,j,h) U(v,i) dv = \frac{\mathcal{R}P_{sr}}{w_2 w_3 M_D}\left\{\frac{w_3 w_2 (K-1)(M-1)}{(M_D N_D P_s - 1)} + \frac{w_3 (K-1)(N-1)(M-1)}{(M_D N_D P_s - 1)}\right\} \quad (13)$$

$$I_3 = \mathcal{R}\int_0^\infty G_3(v)dv = \int_0^\infty \frac{\mathcal{R}P_{sr}}{(w_1 - 1)(w_2 - 1) w_2 w_3 \Delta v} \times \sum_{k=1}^{K} d(k) R^{(3)}(i,j,h) U(v,i) dv = \frac{\mathcal{R}P_{sr}}{w_2 w_3 M_D}\left\{+\frac{w_3 (K-1)(N-1)(M-1)}{(M_D N_D P_s - 1)}\right\} \quad (14)$$

Where $\mathcal{R}$ is the responsivity of the photodiode. The average output photocurrent is :-

$$I_r = \mathcal{R}\int_0^\infty \{[G_0(v) - G_2(v)] - [G_1(v) - G_3(v)]\}dv = [I_0 - I_1 - I_2 + I_3] = \frac{\mathcal{R}P_{sr} w_1}{M_D} \quad (15)$$

The variance of the *PIIN* current is shown below:

$$\langle i^2_{PIIN} \rangle = B_w \mathcal{R}^2 I_r^2 \tau_r = B_w \mathcal{R}^2 I_r^2 \frac{\int_0^\infty [G_0(v) - G_1(v) - G_2(v) + G_3(v)]^2 dv}{\left\{\int_0^\infty [G_0(v) - G_1(v) - G_2(v) + G_3(v)]\, dv\right\}^2} = B_w \mathcal{R}^2 \int_0^\infty [G_0(v) - G_1(v) - G_2(v) + G_3(v)]^2 dv \quad (16)$$

Since $G_0(v)$ and $G_1(v)$ do not overlap with $G_2(v)$ and $G_3(v)$, so that $< i^2_{PIIN} >$ is:

$$\langle i^2{}_{PIIN}\rangle = B_w\mathcal{R}^2 \int_0^\infty [G_0^2(v) + G_1^2(v) + G_2^2(v) + G_3^2(v) - 2G_0(v)G_1(v) - 2G_2(v)G_3(v)]dv \quad (17)$$

First, we find the integral of each part as follows:

$$\int_0^\infty G_0^2(v)dv = \frac{P_{sr}^2}{w_2^2 w_3^2 \Delta v^2} \times \int_0^\infty \left[\sum_{k=1}^{K} R^{(0)}(i,j,h)U(v,i)\right]^2 dv = \frac{M_D I_0^2}{\Delta v\, w_1 \mathcal{R}^2} \quad (18)$$

$$\int_0^\infty G_1^2(v)dv = \frac{P_{sr}^2}{(w_2-1)^2 w_3^2 w_2^2 \Delta v^2} \times \int_0^\infty \left[\sum_{k=1}^{K} R^{(1)}(i,j,h)U(v,i)\right]^2 dv = \frac{M_D I_1^2}{\Delta v\, w_1 \mathcal{R}^2} \quad (19)$$

$$\int_0^\infty G_2^2(v)dv = \frac{P_{sr}^2}{(w_1-1)^2 w_3^2 w_2^2 \Delta v^2} \times \int_0^\infty \left[\sum_{k=1}^{K} R^{(2)}(i,j,h)U(v,i)\right]^2 dv = \frac{M_D I_2^2}{\Delta v\, (w_1-1)^2 \mathcal{R}^2} \quad (20)$$

$$\int_0^\infty G_3^2(v)dv = \frac{P_{sr}^2}{(w_2-1)^2 (w_1-1)^2 w_3^2 w_2^2 \Delta v^2} \times \int_0^\infty \left[\sum_{k=1}^{K} R^{(3)}(i,j,h)U(v,i)\right]^2 dv = \frac{M_D I_3^2}{\Delta v\, (w_1-1)^2 \mathcal{R}^2} \quad (21)$$

$$\int_0^\infty G_0(v)G_1(v)dv = \frac{P_{sr}^2}{(w_2-1)w_2^2 w_3^2 \Delta v^2} \times \int_0^\infty \left[\sum_{k=1}^{K} R^{(0)}(i,j,h)U(v,i)\right] \times \left[\sum_{k=1}^{K} R^{(1)}(i,j,h)U(v,i)\right] dv = \frac{M_D I_0 I_1}{\Delta v\, w_1 \mathcal{R}^2} \quad (22)$$

$$\int_0^\infty G_2(v)G_3(v)dv = \frac{P_{sr}^2}{(w_1-1)^2 (w_2-1) w_2^2 w_3^2 \Delta v^2} \times \int_0^\infty \left[\sum_{k=1}^{K} R^{(2)}(i,j,h)U(v,i)\right] \times \left[\sum_{k=1}^{K} R^{(3)}(i,j,h)U(v,i)\right] dv = \frac{M_D I_2 I_3}{\Delta v\, (w_1-1)^2 \mathcal{R}^2} \quad (23)$$

Substitute equs.(18-23) into equ.(17) when all users send bit '1' we can present the *PIIN* as:

$$\begin{aligned}\langle i^2{}_{PIIN}\rangle &= B_w\mathcal{R}^2 I_r^2 \tau_r \\ &= B_w\mathcal{R}^2 \left\{\frac{M_D I_0^2}{\Delta v\, w_1 \mathcal{R}^2} + \frac{M_D I_1^2}{\Delta v\, w_1\, \mathcal{R}^2} + \frac{M_D I_2^2}{\Delta v\, (w_1-1)^2\, \mathcal{R}^2} + \frac{M_D I_3^2}{\Delta v\, (w_1-1)^2\, \mathcal{R}^2} + \frac{M_D I_0 I_1}{\Delta v\, w_1\, \mathcal{R}^2} + \frac{M_D I_2 I_3}{\Delta v\, (w_1-1)^2\, \mathcal{R}^2}\right\} \\ &= \frac{M_D B_w}{\Delta v}\left\{\frac{(I_0-I_1)^2}{w_1} + \frac{(I_2-I_3)^2}{(w_1-1)^2}\right\}\end{aligned} \quad (24)$$

Because of the probability of sending bit '1' or '0' is 0.5 for each user, the $< i^2_{PIIN} >$will be:

$$\langle i^2{}_{PIIN}\rangle = \frac{M_D B_w}{2\Delta v}\left\{\frac{(I_0-I_1)^2}{w_1} + \frac{(I_2-I_3)^2}{(w_1-1)^2}\right\} \quad (25)$$

Then$< i^2_{shot} >$ with 0.5 probability of sending '1' or '0' can be expressed:

$$\begin{aligned}\langle i^2{}_{shot}\rangle &= 2eB_w I_{total}/2 \\ &= eB_w(I_0 + I_1 + I_2 + I_3) \\ &= eB_w \frac{\mathcal{R}P_{sr}}{w_2 w_3 M}\left\{w_3 w_1 w_2 + \frac{2w_2 w_3 (K-1)(M-1)}{(M_D N_D P_s - 1)} + \frac{2w_3 w_1 (K-1)(N-1)}{(M_D N_D P_s - 1)} + \frac{4w_3 (K-1)(N-1)(M-1)}{(M_D N_D P_s - 1)}\right\},\end{aligned} \quad (26)$$

and the variance of thermal noise current is:

$$\langle i^2{}_{thermal}\rangle = \frac{4K_b T_n B_w}{R_L} \quad (27)$$

The average signal to noise ratio *SNR* can be obtained based on the equs. (15), (25), (26) and(27) as in equ. (28):

$$SNR = \frac{I_r^2}{\langle i^2{}_{PIIN}\rangle + \langle i^2{}_{shot}\rangle + \langle i^2{}_{thermal}\rangle}$$

$$SNR = \frac{\left(\frac{\mathcal{R}P_{sr}w_1}{M_D}\right)^2}{\frac{M_D B_w}{2\Delta v}\left\{\frac{(I_0-I_1)^2}{w_1} + \frac{(I_2-I_3)^2}{(w_1-1)^2}\right\} + eB_w(I_0 + I_1 + I_2 + I_3) + \frac{4K_b T_n B_w}{R_L}} \quad (28)$$

Then the BER can be expressed as in [6]:

$$BER = \frac{erfc\left(\sqrt{\frac{SNR}{8}}\right)}{2}, \quad (29)$$

Where

$$erfc(z) = \frac{2}{\sqrt{\pi}} \int_z^{\infty} \exp(-y^2)\, dy. \quad (30)$$

TABLE 3. The parameters used in the numerical calculations

Symbol	$\mathcal{R}$	P_{sr}	Δv	λ_0	T_n	R_L
Value	0.75	-7 dBm	5THz	1550 nm	300 K	1030 Ω

Numerical Results

The performance of the 3-D PD/MD code with $(M_D = 4*3, N_D = 3*3, Ps = 13)$ and the previously presented 2-D PD, 2-D DPD and 3-D PD codes for the same number of total users in the presence of the PIIN, the photodiode shot noise, and the thermal noise are illustrated in Fig.3 and Fig.4 for a data rate of 0.622Gbps and 1.25Gbps respectively. The system parameters used in the numerical analysis are presented in TABLE 3. The receiver electrical bandwidth B_w was chosen as half of the data rate for the 2-D PD and 2-D DPD code while it is 0.5*N and 0.5*N_D of the data rate for the 3-D PD and 3-D DPD/MD codes, respectively.

The relationship between the BER and the number of active users K for the all mentioned codes with the data bit rate of 0.622Gbps is drawn in Fig.3. The Figure illustrates that the performance of the 3-D DPD/MD code is much better than the others. At BER of (10^{-9}) the 3-D DPD/MD code can accommodate 1000 users in comparison to 650 users for the 3-D PD code in which it achieves a cardinality enhancement by 53%.

In addition to that, Fig. 4 shows the same relation at a data bit rate of 1.25Gbps. The figure demonstrates that the systems performance of all codes degrade with increasing the data rate due to the increasing of PIIN and shot noises. Although, the 3-D DPD/MD code achieves more active users. At BER of (10^{-9}) the 3-D DPD/MD code can accommodate 100 users more than the 3-D PD code. Therefore, the system with the 3-D DPD/MD code has a superior performance compared with others.

The relation between the *BER* and the effective received power in dBm at the data bit rate equal to 0.622Gbps and the number of active users is 600 for different codes is shown in Fig. 5. The poor performance at low power level for all systems because the domination of the static thermal noise power that exceed the received power. At power level of middle and high, the 3-D DPD/MD code gives better performance due to its' ability to reduce the PIIN and shot noises with a short code length. It is obvious that the proposed code requires the minimum power at BER of 10^{-9} where the 3-D PD incurs a power penalty of about 5 dB. Therefore, it can be concluded that the proposed code is reliable for a low power transmission.

Fig. 6 illustrates the BER versus the data rate of each user for all codes under the comparison when the number of active users is 600 and the effective power is -7 dBm. It is obvious that the 3-D DPD/MD code supports 600 active users with the highest data rate compared to other codes at free error.

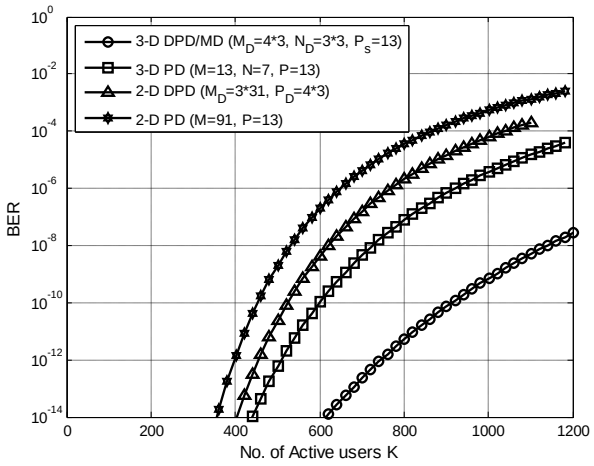

Fig.3. The *BER* versus the number of active users of 3-D DPD/MD code with $(M_D = 4*3, N_D = 3*3, P_S = 13)$ when the effective power P_{sr}=-7dBm and data rate is 0.622Gbps

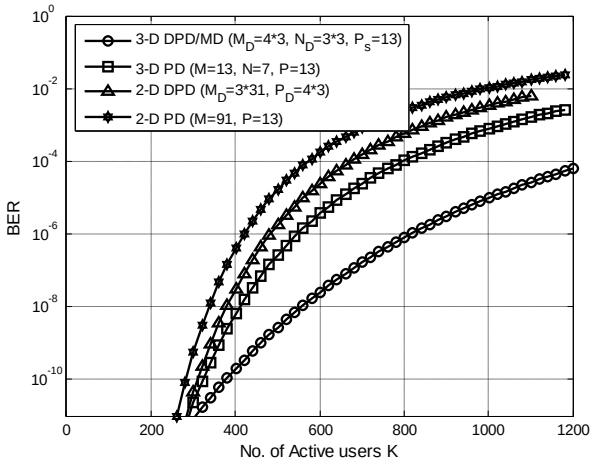

Fig.4. The *BER* versus the number of active users of 3-D DPD/MD code with $(M_D = 4*3, N_D = 3*3, P_S = 13)$ when the effective power P_{sr}=-7dBm and data rate is 1.25Gbps

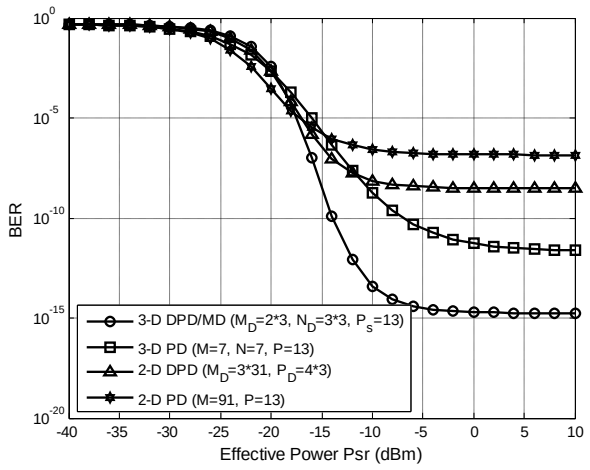

Fig.5. The *BER* versus the effective power P_{sr} of 3-D DPD/MD code with $(M_D = 4 * 3, N_D = 3 * 3, P_S = 13)$ when the number of active users is 600 and data rate is 0.622Gbps.

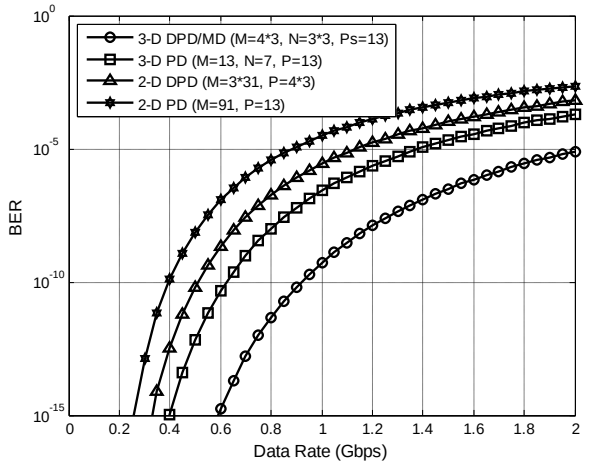

Fig.6. The *BER* versus the data rate of 3-D DPD/MD code with $(M_D = 4 * 3, N_D = 3 * 3, P_S = 13)$ when the number of active users is 600 and P_{sr}=-7dBm.

Conclusion

In this Paper, a new three-dimensional code referred as 3-D DPD/MD code is proposed for the spectral/time/spatial OCDMA system. The construction of this code based on the MD code and the PD code with the dilution method. The performance of the OCDMA system with the proposed code has been investigated by using the numerical analysis. The effects of the PIIN, shot noise and the thermal noise were taken into account during the investigation process. Based on the comparison with recent codes, the numerical results for the 3-D DPD/MD code shows that this code can significantly reduce the effect of the receiver noises and give a low BER for a large number of active users and high data rate, so this code is succeed in improvement of the system performance.

References

[1] F. R. K. Chung, J. Salehi, and V. K. Wei, "Optical orthogonal codes: design, analysis and applications," *Inf. Theory, IEEE Trans.*, vol. 35, no. 3, pp. 595–604, 1989.

[2] G.-C. Yang and W. C. Kwong, "Performance analysis of optical CDMA with prime codes," *Electron. Lett.*, vol. 31, no. 7, pp. 569–570, 1995.

[3] C. S. Weng and J. Wu, "Perfect difference codes for synchronous fiber-optic CDMA communication systems," *J. Light. Technol.*, vol. 19, no. 2, pp. 186–194, 2001.

[4] D. Zaccarin and M. Kavehrad, "An optical CDMA system based on spectral encoding of LED," *Photonics Technol. Lett. IEEE*, vol. 5, no. 4, pp. 479–482, 1993.

[5] M. Kavehrad and D. Zaccarin, "Optical code-division-multiplexed systems based on spectral encoding of noncoherent sources," *Light. Technol. J.*, vol. 13, no. 3, pp. 534–545, 1995.

[6] Z. Wei, H. M. H. Shalaby, and H. Ghafouri-Shiraz, "Modified quadratic congruence codes for fiber Bragg-grating-based spectral-amplitude-coding optical CDMA systems," *Light. Technol. J.*, vol. 19, no. 9, pp. 1274–1281, 2001.

[7] Z. Wei and H. Ghafouri-Shiraz, "Unipolar codes with ideal in-phase cross-correlation for spectral amplitude-coding optical CDMA systems," *Commun. IEEE Trans.*, vol. 50, no. 8, pp. 1209–1212, 2002.

[8] Z. Wei and H. Ghafouri-Shiraz, "Codes for spectral-amplitude-coding optical CDMA systems," *J. Light. Technol.*, vol. 20, no. 8, p. 1284, 2002.

[9] T. H. Abd, S. A. Aljunid, H. A. Fadhil, R. A. Ahmad, and N. M. Saad, "Development of a new code family based on SAC-OCDMA system with large cardinality for OCDMA network," *Opt. Fiber Technol.*, vol. 17, no. 4, pp. 273–280, 2011.

[10] C.-C. Yang and J.-F. Huang, "Two-dimensional M-matrices coding in spatial/frequency optical CDMA networks," *Photonics Technol. Lett. IEEE*, vol. 15, no. 1, pp. 168–170, 2003.

[11] C. H. Lin, J. Wu, and C. L. Yang, "Noncoherent spatial/spectral optical CDMA system with two-dimensional perfect difference codes," *J. Light. Technol.*, vol. 23, no. 12, pp. 3966–3980, 2005.

[12] H. Yin, L. Ma, H. Li, and L. Zhu, "A new family of 2D wavelength/time codes with large cardinality for incoherent spectral amplitude coding OCDMA networks and analysis of its performance," *Photonic Netw. Commun.*, vol. 19, no. 2, pp. 204–211, 2009.

[13] B.-C. Yeh, C.-H. Lin, C.-L. Yang, and J. Wu, "Noncoherent spectral/spatial optical CDMA system using 2-D diluted perfect difference codes," *J. Light. Technol.*, vol. 27, no. 13, pp. 2420–2432, 2009.

[14] B. Yeh, C. Lin, J. Wu, and L. Fellow, "Noncoherent Spectral / Time / Spatial Optical CDMA System Using 3-D Perfect Difference Codes," vol. 27, no. 6, pp. 744–759, 2009.